Journal of Inflammation Research Dovepress

Open Access Full Text Article ORIGINAL RESEARCH

Molecular Differences in Glomerular Compartment to Distinguish Immunoglobulin A Nephropathy and Lupus Nephritis

Haidong Zhang[1], Sicong Li[2], Zhenling Deng[1], Yue Wang[1]

[1]Department of Nephrology, Peking University Third Hospital, Beijing, 100191, People's Republic of China; [2]School of Pharmaceutical Sciences, Peking University, Beijing, People's Republic of China

Correspondence: Yue Wang; Zhenling Deng, Email bjwangyue@sina.com; dengzhenling1985@126.com

Background: Immunoglobulin A nephropathy (IgAN) and lupus nephritis (LN) are the most prevalent primary and secondary glomerular diseases, respectively, with several similarities in clinical presentations. Common pathogenic mechanisms in IgAN and LN have been well investigated by previous studies. However, the manifestation mechanism of these two independent diseases carrying distinct immunofluorescent pathological features is still unknown considering the similarities between them. Therefore, differences in pathogenic mechanisms between IgAN and LN were compared in this study.

Methods: R packages were used for processing the glomerular gene expression datasets acquired from the Gene Expression Omnibus (GEO) database. Least Absolute Selection and Shrinkage Operator (LASSO) and multivariate logistic regression analysis were used to construct models predicting IgAN and LN. Cibersort was used to process the immune cell infiltration analysis. Immunochemistry was used to validate the findings by bioinformatics analysis.

Results: In the predicting models based on differentially expressed genes (DEG) and weighted correlation network analysis (WGCNA), retinoic acid receptor γ (RARG) and prolactin releasing hormone (PRLH) were independent risk factors for IgAN, and HECT domain and RCC1-like domain-containing protein 5 (HERC5) and interferon stimulated exonuclease gene 20 (ISG20) were independent risk factors for LN. Gene Ontology (GO) analysis revealed that DEGs mostly correlated to IgAN were enriched in ligand-receptor activity-induced cellular growth and development, while DEGs mostly correlated to LN were enriched in nucleic acid/nucleotide binding-induced type I interferon-related activity and response to virus infection. Immune infiltration analysis showed CD4+ T-cells and M2 macrophage abundance in the glomerular compartment in IgAN and LN, respectively. Immunochemistry validated the predicting models for IgAN and LN and revealed different expression patterns of RARG, PRLH, HERC5, and ISG20.

Conclusion: We investigated key differences in the pathogenesis between IgAN and LN and provided validated predicting models to distinguish IgAN and LN. RARG and PRLH, HERC5 and ISG20 might play an essential role in the formation of IgAN and LN, respectively.

Keywords: immunoglobulin A nephropathy, lupus nephritis, pathogenic difference, nomogram, immune infiltration, biomarker

Introduction

Chronic kidney disease is a common cause of end-stage renal disease (ESRD) affecting global public health significantly. IgAN and LN are the most prevalent primary and secondary glomerular diseases, respectively,[1,2] with similar clinical manifestations, such as hematuria and proteinuria,[3,4] and several similarities in their pathogenesis and pathological presentation. As autoimmune kidney diseases, intrarenal immune complex deposition was detected by immunofluorescence in both IgAN and LN. Complement elements activation,[5,6] inflammatory cells infiltration including T cells[7,8] and macrophages,[9,10] and Toll-like receptors (TLRs),[11,12] important members in response to infection in innate immunity, were investigated to be involved in enhancing and deteriorating intrarenal inflammation in both IgAN and LN. Mesangial hypercellularity is common in IgAN, and diffuse mesangial hypercellularity was found in about 20% to 40% of IgAN patients.[13,14] Significant mesangial hypercellularity could also be found in class II, class III, class IV LN, and class II LN

Received: 23 September 2024
Accepted: 14 December 2024
Published: 21 December 2024

(mesangial proliferative) accounts for 7–22% of all cases.[4] Though prodromic infection in IgAN and positive results of antinuclear antibody profile in LN could help distinguish IgAN patients from LN patients clinically, it is still difficult to distinguish IgAN from LN in the pathological aspect in these patients with mesangial hypercellularity.

IgAN and LN are two independent kidney diseases carrying different immunofluorescent pathological features. Pathological lesions of IgAN are characterized by polymeric Gd-IgA1 containing immune complex deposition in mesangium with expansion of extracellular matrix and mesangial hypercellularity, while LN is characterized by full field of IgA, IgM, and IgG deposition with different histological classes in kidney biopsies.[15,16] Gd-IgA1 deposition induced proliferation and activation of mesangial cells plays the key role in the pathogenesis of IgAN,[17] followed by altered mesangial – endothelial/podocyte/tubular epithelial cell crosstalk[18,19] deteriorating renal tissue damage. Compared to IgAN, endogenous nuclear particles from renal cells and autoantibodies targeting these endogenous antigens by misidentifying them as viral antigens combined to form immune complexes, initiating intrarenal inflammation in LN.[20] Different types of antigens seemed to induce different histological classes of LN.[15]

Considering all those similarities between IgAN and LN, it is confusing how these two independent diseases carrying distinct immunofluorescent pathological features are manifested, and the mechanism under which different phenotypic changes are associated with these two diseases remains to be elucidated. Though several studies have investigated the pathogenesis and biomarkers of IgAN[21–23] and LN[24–27] by using bioinformatics analysis, only Jia[28] compared genetic susceptibility loci in IgAN and LN by genome-wide association studies (GWAS) enrichment analysis. Studies focusing on comparing different pathogenesis between IgAN and LN are still lacking.

Therefore, we explored the key differences in the pathogenesis between IgAN and LN by acquiring glomerular expression profiles available in public databases in this study to elucidate different mechanisms underlying the pathogenesis of IgAN and LN.

Method

Data Source

Gene expression datasets from expression profiling by array based on human samples were searched in the GEO database (http://www.ncbi.nlm.nih.gov/geo) using “IgA nephropathy”, “lupus nephritis”, and “glomerular compartment” as keywords. Expression data of 26 IgAN patients and 30 LN patients were extracted from the GSE99339 dataset. As the GSE99339 dataset did not consist of healthy controls, expression data of 22 healthy controls (HCs) from the GSE93798 dataset were extracted for data integration and further comparison.

Data Integration and Identification of DEGs

The R package Sva was used to integrate gene expression data of IgAN patients, LN patients, and HCs in the two aforementioned datasets into the gene expression profile of the renal glomerulus, in which the batch effect was adjusted. Probe sets without a corresponding gene symbol were removed, and genes with multiple probe sets were averaged. Then R package Limma was used to determine the DEGs between IgAN patients and healthy controls, and between LN patients and healthy controls. Statistical significance for the DEGs was considered with a $P < 0.05$ and a |fold change (FC)| ≥ 1, and $FC \geq 1$ and $FC \leq -1$ were used to indicate upregulated and downregulated DEGs, respectively. Volcano maps were drawn using the R package ggplot2. To identify common DEGs with the same and opposite altered trends between IgAN patients and LN patients, the Venn online tool was used to draw a Venn map.

Weighted Correlation Network Analysis

The WGCNA R package (version 1.68) was used for the WGCNA of the integrated gene expression profile of the renal glomerulus (The R code could be freely available at: https://github.com/cran/WGCNA). The soft threshold power in this study was chosen as 8 ($R^2 = 0.9$) for the correlation matrix, calculated by pickSoftThreshold of the WGCNA package. The soft threshold power and gene correlation matrix were used to build an adjacency matrix, from which the topological overlap matrix (TOM) and the dissimilarity TOM (1-TOM) were transformed. TOM was then used to measure gene expression similarity, and genes were hierarchically clustered and visualized in a dendrogram according to the 1-TOM.

The first principal component of each gene module was used to determine module eigengenes (MEs) to represent all genes in each module. Correlations between clinical features (IgA nephropathy, lupus nephritis, or healthy control) and MEs were then analyzed for IgAN and LN-associated modules, in which the gene significance (GS) and the module membership (MM) were used to identify the modules. Correlations between MM and GS were analyzed to determine modules of interest. Genes mostly correlated to IgAN and LN were determined with MM > 0.8 and GS > 0.2 in the associated modules, respectively.

Diagnostic Value of the Correlated Genes with Significant Differential Expression in IgAN - and LN - Associated Modules

The Venn online tool was used to identify DEGs mostly correlated to IgAN and LN in the IgAN - and LN-associated modules by intersecting genes mostly correlated to IgAN and LN in the associated modules with DEGs. Statistical analysis of the diagnostic value of those DEGs mostly correlated to IgAN and LN was processed by R software. We extracted the expression data of those DEGs mostly correlated to IgAN and LN from the glomerular profile, and LASSO regression analysis was utilized to select the genes with optimal predictive capability in IgAN and LN. Multivariate logistic regression analysis was utilized to identify the independent factors by incorporating the genes selected in the LASSO regression. Stepwise logistic regression would be performed if there was strong multicollinearity ($r > 0.8$) between DEGs mostly correlated to IgAN and LN measured by Spearman's rank correlation tests. Models were constructed to predict IgAN and LN by developing nomograms based on the independent factors with a two-sided p-value of <0.05 in the logistic regression. The models' performance was measured by the area under the receiver operating characteristic curve (AUC), concordance index (C-index), sensitivity, and specificity. The nomogram was subjected to 100 bootstrap resamples for internal validation to assess their predictive accuracies. The calibration curve measured the consistency between the observed outcomes and predicted probabilities. The net clinical benefit was measured by decision curve analysis (DCA).

Functional Enrichment Analysis and Protein–Protein Interaction (PPI) Network Construction

GO and Kyoto Encyclopedia of Genes and Genomes (KEGG) enrichment analyses run by the "clusterProfiler" R package were utilized to functionally annotate DEGs mostly correlated to IgAN and LN. P.adjust value <0.05 and a false discovery rate (FDR) <0.25 in the GO and KEGG enrichment were considered statistically significant.

The online search tool STRING (http://string-db.org) was used to investigate the interaction among DEGs with opposite altered trends in IgAN and LN to construct PPI networks, respectively. Interactions with a combined score of over 0.4 were considered statistically significant. Then, the Cytoscape software was utilized to visualize the PPI network and examine major functional modules, with the following selection criteria: K-core = 2, degree cutoff = 2, max depth = 100, and node score cutoff = 0.2.

Estimation of Immune Cell Infiltration and Investigation of Its Correlation with Risk Factor Genes in IgAN and LN

To evaluate immune cell infiltration in IgAN and LN, the gene expression matrix data was uploaded to CIBERSORT (https://cibersort.stanford.edu/) to obtain the immune cell infiltration matrix of the 22 kinds of immune cells. Violin diagrams to visualize the differences in immune cell infiltration among IgAN patients, LN patients, and HCs were drawn by the R package "ggplot2". Spearman's rank correlation tests were used to investigate the correlation between risk factor genes in the nomograms and the abundances of infiltrating immune cells in IgAN and LN.

Immunohistochemistry

Immunohistochemistry (IHC) staining was carried out to validate the findings in predicting IgAN and LN. Paraffin-embedded tissues of IgAN and LN used for IHC were gained from the Department of Nephrology, Peking University Third Hospital, Beijing. Sections were boiled in Tris/EDTA buffer (pH 9.0) for antigen retrieval (ZLI-9069; ZSGB-BIO,

China), and endogenous HRP activity was blocked with 3% H2O2. After blockage with bovine serum albumin (ZLI-9056; ZSGB-BIO, China), sections were incubated with primary antibodies against RARG (11424-1-AP, rabbit; 1:800, proteintech, USA), PRLH (YN3961, rabbit; 1:500, Immunoway, USA), ISG20 (22,097-1-AP, rabbit; 1:1000, proteintech, USA), HERC5 (22,692-1-AP, rabbit; 1:300, proteintech, USA) under 4°C overnight. Then, the targets were detected using a two-step detection kit (PV-6000; ZSGB-BIO, China), and the antibody reaction was visualized by 3, 30-diaminobenzidine (DAB) (ZLI-9018; ZSGB-BIO, China). Expression was calculated by intraglomerular mean IHC optical density (OD) score via the use of the Image J software IHC Profiler plugin. Then the obtained mean OD scores were subjected to statistical analysis by GraphPad Prism 8.0.2. The statistical significance ($P \leq 0.05$) was calculated by the means of the one-way analysis of variance or Kruskal–Wallis test.

Patients Inclusion, Ethics Statement, and Written Informed Consent

Renal biopsies from 10 IgAN patients and 8 LN patients, and para-cancerous renal tissues from 5 renal carcinoma patients were included in this study for IHC validation. As there are several subtypes of morphological changes in IgAN and LN, we chose IgAN and LN patients with mild mesangial hypercellularity and mesangial matrix expansion for comparison (M1 pathological change in IgAN according to the Oxford classification, and class II LN according to the ISN/RPS classification). The pathological features and clinical situation (including blood pressure, hematuria, proteinuria, and serum creatinine) of these patients were listed in the Supplementary Table 1. To avoid the influence of renal carcinoma on the para-cancerous renal tissues as much as possible, para-cancerous renal tissues were obtained from area at least 5 cm away from the tumor boundary.

This study protocol was approved by the Ethics Committee of Peking University Third Hospital, approval number M2022204.

Written informed consents were obtained from IgAN and LN patients to participate in the study if their renal biopsies were used for IHC.

Results

Identification and Analysis of DEGs

Our research methodology roadmap is shown in Figure 1. We constructed a gene expression profile of the renal glomerulus by obtaining and integrating gene expression data from the GSE99339 and the GSE93798 datasets from the GEO database, consisting of samples of 26 IgAN patients, 30 LN patients, and 22 hCs (Supplementary Figure 1). The information of those datasets was given in Supplementary Table 2. In IgAN samples compared with HCs, 1030 upregulated DEGs and 1355 downregulated DEGs were identified. In addition, 772 upregulated DEGs and 901 downregulated DEGs were identified in the LN samples compared with HCs (Figure 2a and b). A Venn diagram (Figure 2c) revealed that IgAN and LN shared 735 common DEGs, 11 of which expressed in the same trend, while the other 724 common DEGs expressed in the opposite trend. In those DEGs with the same expression trend in IgAN and LN, 4 of them were upregulated, and the remaining 7 DEGs were downregulated. In those DEGs with the opposite expression trend between IgAN and LN, 392 of them were upregulated in IgAN but downregulated in LN, while the other 332 DEGs were upregulated in LN but downregulated in IgAN. Supplementary Table 3 demonstrated the aforementioned DEGs in detail.

Weighted Co-Expression Network Construction and Correlated Genes Identification

By using 8 as the soft threshold power (Figure 3a), a total of 23 modules were identified in the glomerular profile through the WGCNA, with each color representing a different module in the hierarchical cluster analysis (Figure 3b). Then, a heatmap was mapped for module–trait relationships to evaluate the association between each module and the clinical features (IgAN and LN) according to the Spearman correlation coefficient (Figure 3c). The “salmon” module (r=0.59, p=1.1e-8) was positively associated with IgAN with 8 identified genes mostly correlated to IgAN. The “red” module (r=0.74, p=1.5e-14) and the “green” module (r=0.59, p=1.7e-8) were found positively correlated with LN, including 40 and 35 genes mostly correlated to LN, respectively.

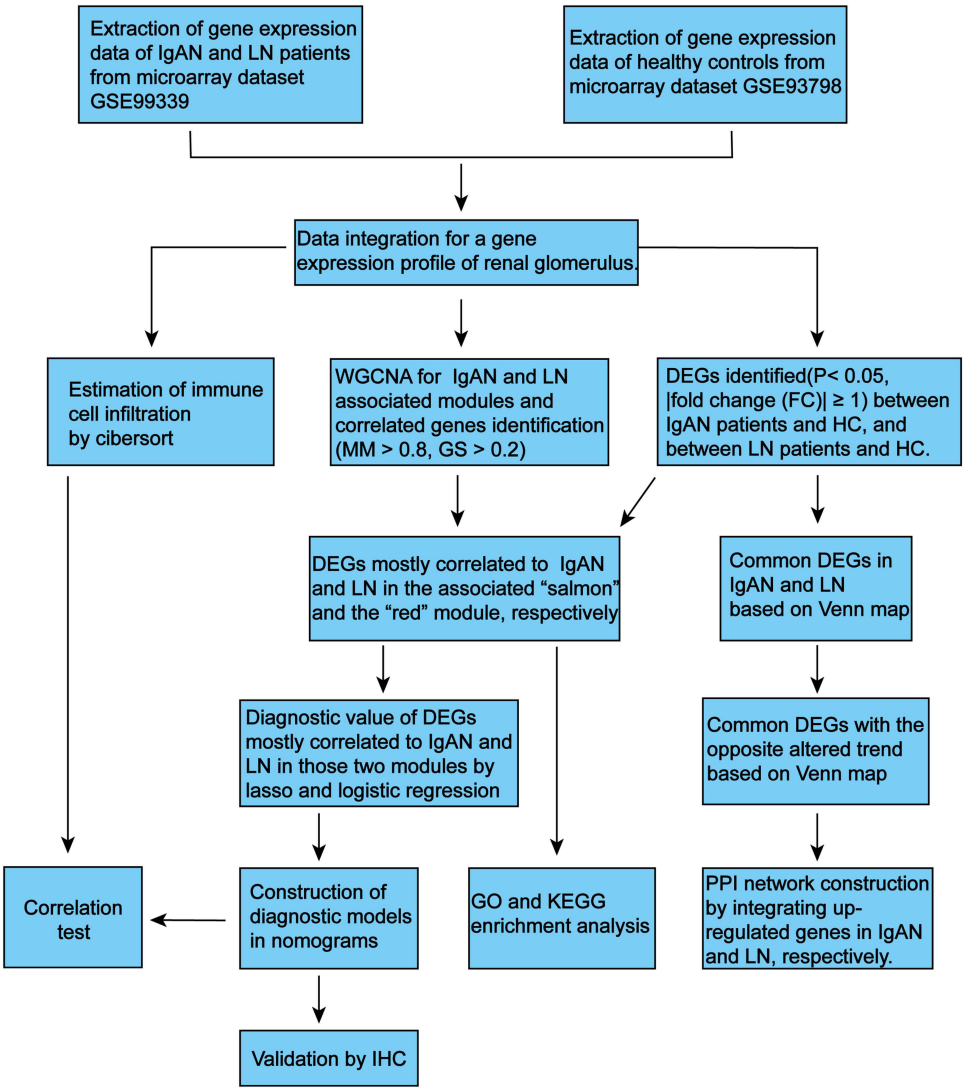

Figure 1 Research design flowchart.
Abbreviations: IgAN, immunoglobulin A nephropathy; LN, lupus nephritis; WGCNA, weighted correlation network analysis; DEG, differentially expressed gene; FC, fold change; MM, module membership; GS, gene significance; HC, healthy control; GO, Gene Ontology; KEGG, Kyoto Encyclopedia of Genes and Genomes; PPI, protein–protein interaction; IHC, immunohistochemistry.

Construction and Internal Validation of Nomograms for IgAN and LN

We obtained intersection elements between genes mostly correlated to IgAN and LN in the associated modules and DEGs and identified DEGs mostly correlated to IgAN and LN by the Venn tool. Five genes in the "salmon" module, 38 genes in the "red" module and 27 genes in the "green" module were identified to be DEGs mostly correlated to IgAN and LN (Supplementary Table 4), respectively. Expression data of all the 5 above genes in the "salmon" module in IgAN patients and HCs and the top 15 above genes ranked by GS in the "red" module in LN patients and healthy controls were extracted from the glomerular profile to construct models by LASSO regression analysis and logistic analysis to predict IgAN and LN, respectively. After the LASSO regression selection, two genes, RARG and PRLH, remained significant predictors for IgAN (Supplementary Figure 2a and b), and three genes, HERC5, HERC6, and ISG20, remained predictors for LN (Supplementary Figure 2c and d). As HERC5 and HERC6 demonstrated strong multicollinearity (Supplementary Figure 3b), stepwise logistic regression was performed for LN. In the end, RARG and PRLH were independent risk factors for IgAN, and HERC5 and ISG20 were independent risk factors for LN. The constructed models based on independent risk factors in IgAN and LN were presented as nomograms (Figure 4a and b). The model predicting IgAN yielded an AUC value of 0.797 (95% CI 0.665–0.929) with a C-index of 0.813 in the training set and 0.801 in the

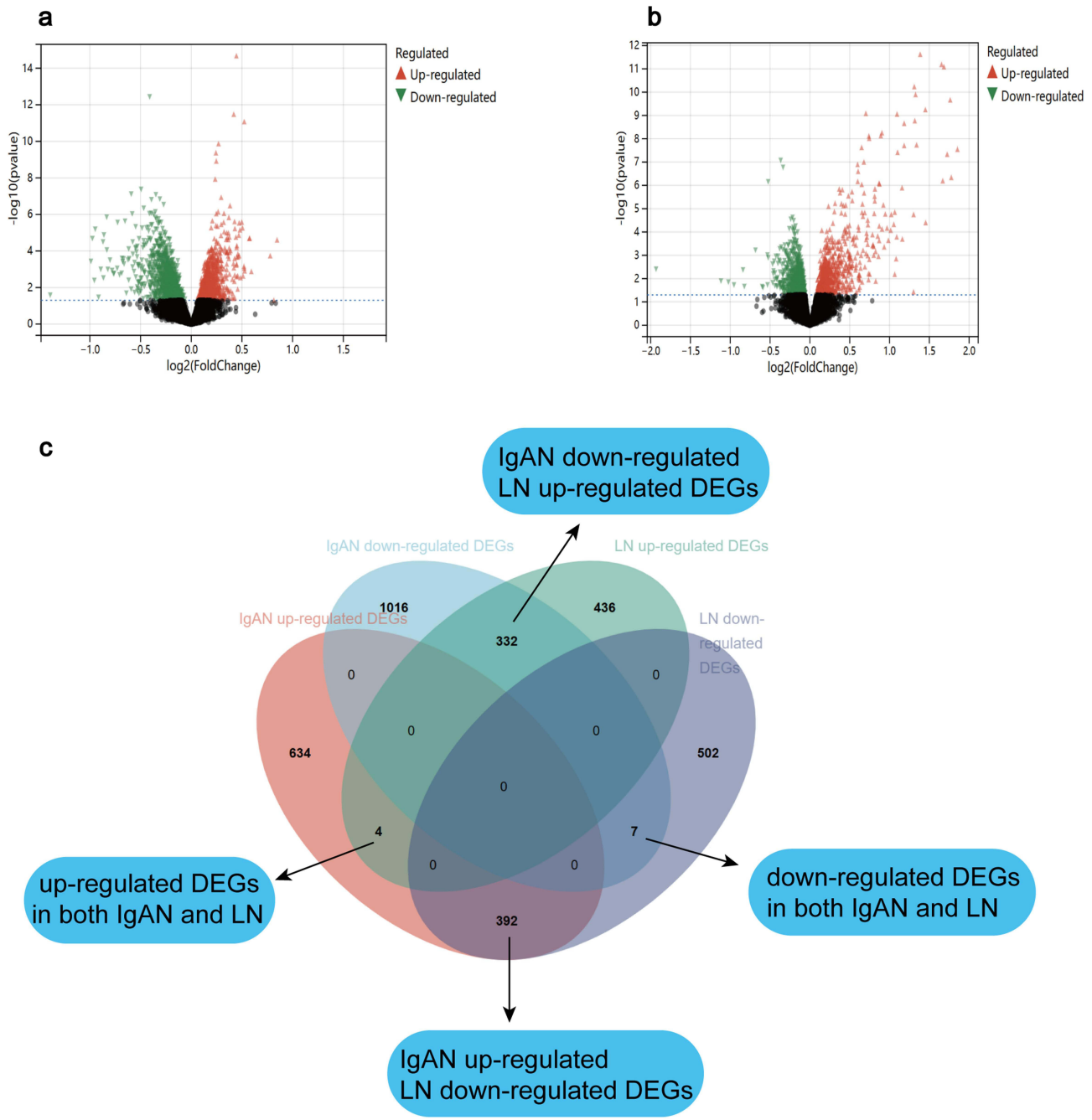

Figure 2 Identification of DEGs between IgAN and HC and between LN and HC, and analysis of the identified DEGs in IgAN and LN based on the expression trend. (**a**) Volcano map demonstrating DEGs between IgAN and HC. (**b**) Volcano map demonstrating DEGs between LN and HC. (**c**) Common DEGs in IgAN and LN with the same expression trend and opposite expression trend.

Abbreviations: IgAN, immunoglobulin A nephropathy; LN, lupus nephritis; HC, healthy control; DEG, differentially expressed gene.

validation set, a sensitivity of 0.731 (95% CI 0.56–0.901) and a specificity of 0.864 (95% CI 0.72–1). And the model predicting the LN yielded an AUC value of 0.992 (95% CI 0.976–1) with a C-index of 0.988 in the training set and 0.989 in the validation set, a sensitivity of 1 (95% CI 1–1) and a specificity of 0.955 (95% CI 868–1). The analysis suggested good performance of both models. The calibration curves of both models demonstrated good consistency between observative outcomes and predicted probabilities (Figure 4c and d). DCA showed that the nomograms had greater net benefits for the identification of IgAN and LN, respectively, than that without the predicting models (Figure 4e and f).

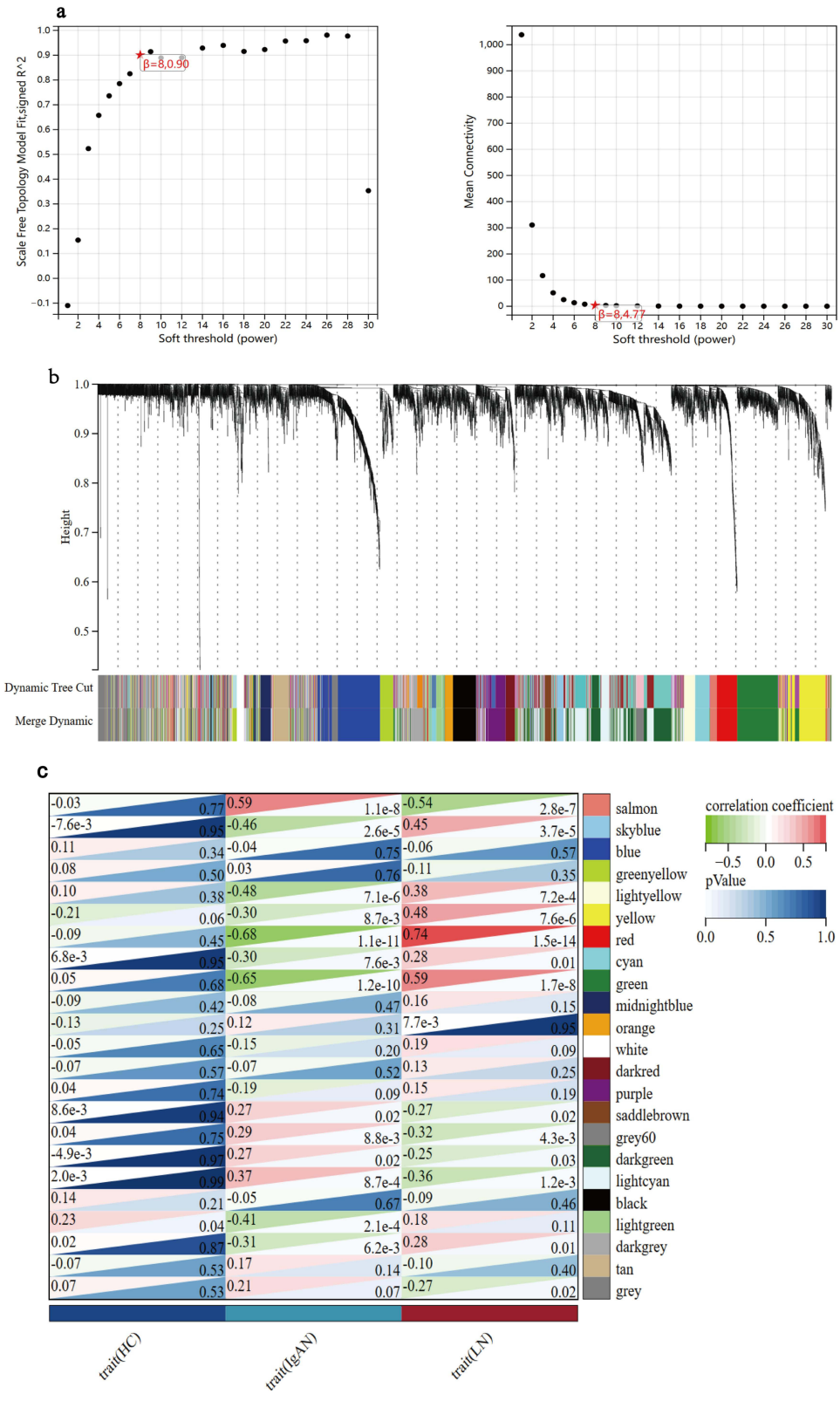

Figure 3 WGCNA of the gene expression profile of renal glomerulus for IgAN and LN. (**a**) Soft thresholding power analysis allowed for provision of scale-free fit index of network topology. (**b**) The cluster dendrogram of co-expression genes in IgAN and LN. (**c**) Module-trait relationships by heatmap in IgAN and LN.
Abbreviations: IgAN, immunoglobulin A nephropathy; LN, lupus nephritis; HC, healthy control; WGCNA, weighted correlation network analysis.

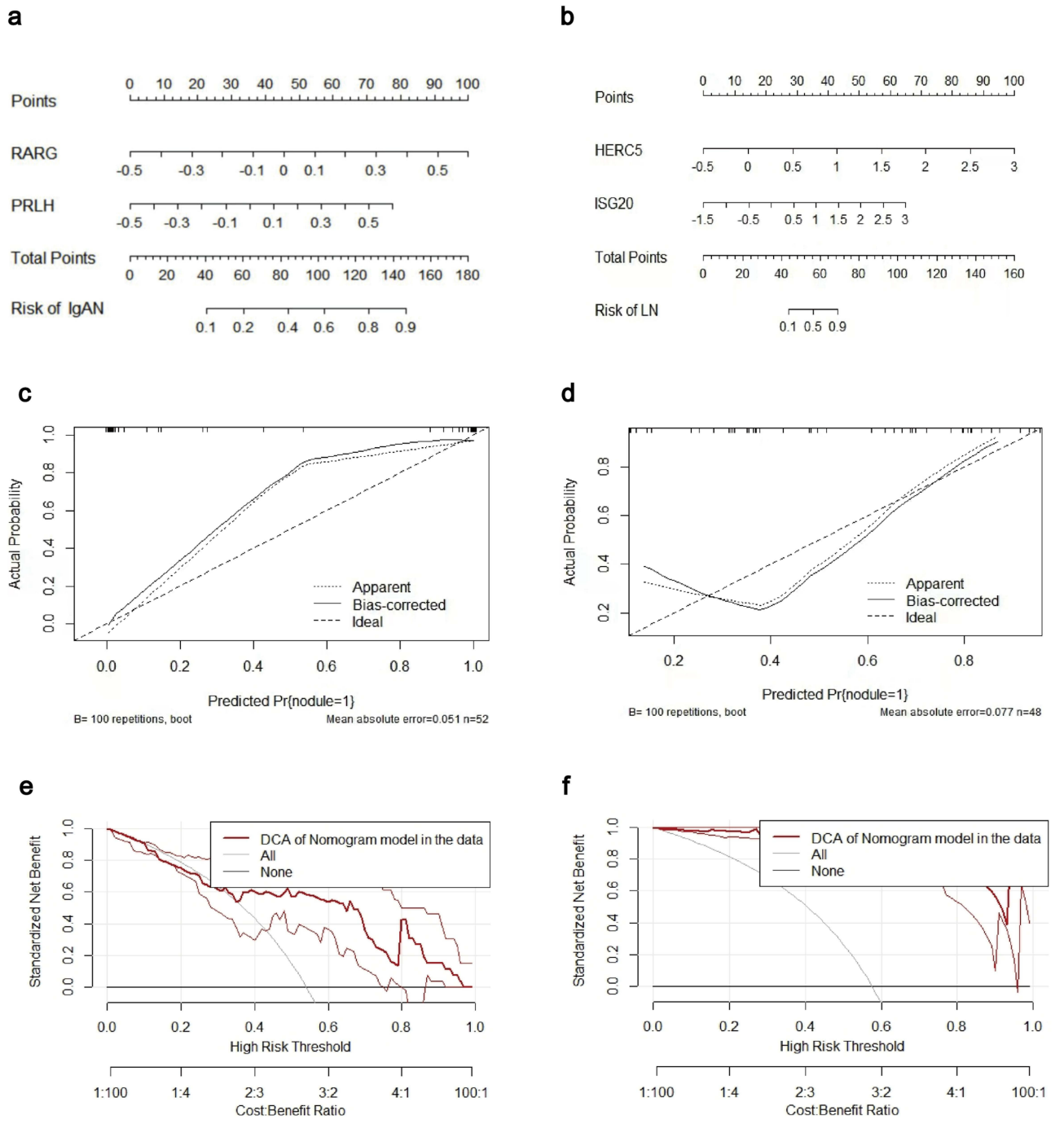

Figure 4 Construction of predicting models for IgAN and LN. (**a**) Nomogram to predict risk of IgAN. (**b**) Nomogram to predict risk of LN. (**c**) Calibration curve of the nomogram predicting IgAN. (**d**) Calibration curve of the nomogram predicting LN. In (**c**) and (**d**), the dashed line represents the original performance, and the solid dashed line represents the performance during internal validation by bootstrapping (B = 40 repetitions). (**e**) Decision curve analysis for the IgAN risk nomogram. (**f**) Decision curve analysis for the LN risk nomogram. The y-axis in (**e**) and (**f**) measures the net benefit.

Abbreviations: IgAN, immunoglobulin A nephropathy; LN, lupus nephritis; RARG, retinoic acid receptor γ; PRLH, prolactin releasing hormone; HERC5, HECT domain, and RCC1-like domain-containing protein 5; ISG20, interferon stimulated exonuclease gene 20; DCA, decision curve analysis.

Functional Enrichment Analysis and PPI Network Construction

Enrichment analysis conducted by the "clusterProfiler" package revealed the biological functions and pathways related to DEGs were mostly correlated to IgAN and LN. Significant enrichments (top 10 in maximum) were listed. GO analysis revealed that the biological function of DEGs mostly correlated to IgAN was mainly enriched in ligand-receptor activity-induced cellular growth and development (Figure 5a), in which the two genes RARG and PRLH in the nomogram

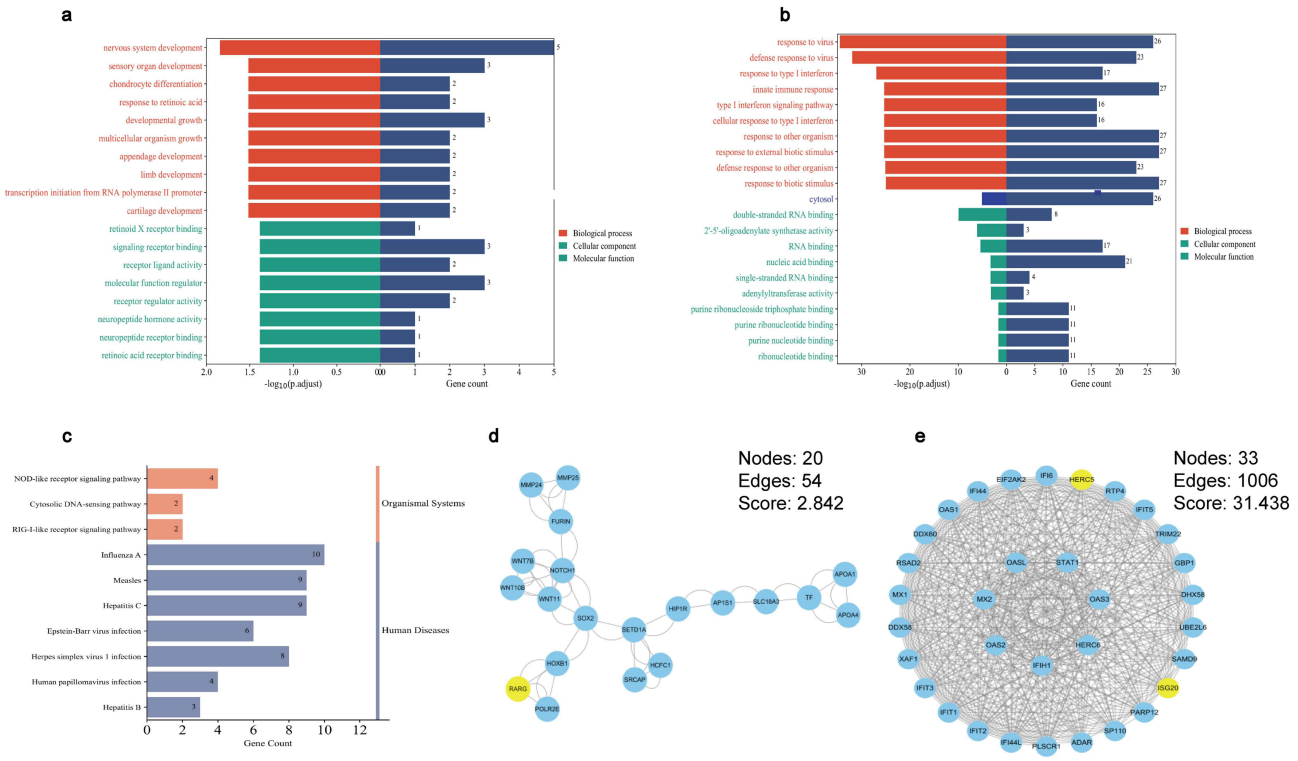

Figure 5 Functional enrichment analysis and PPI networks construction for IgAN and LN. (**a**) GO enrichment analysis of DEGs mostly correlated to IgAN in the "salmon" module. (**b** and **c**) GO and KEGG enrichment analysis of DEGs mostly correlated to LN in the "red" module. (**d**) Significant gene clustering module consisting of DEGs mostly correlated to IgAN in the nomogram for IgAN. (**e**) Significant gene clustering module consisting of DEGs mostly correlated to LN in the nomogram for LN.
Abbreviations: PPI, protein–protein interaction; IgAN, immunoglobulin A nephropathy; LN, lupus nephritis; GO, Gene Ontology; DEG, differentially expressed gene; KEGG, Kyoto Encyclopedia of Genes and Genomes.

predicting IgAN were involved (Supplementary Table 5). And biological function of DEGs is mostly correlated to LN in the "red" module enriched in nucleic acid/nucleotide binding-induced type I interferon-related activity and response to virus infection (Figure 5b), and the two genes HERC5 and ISG20 in the nomogram predicting LN were involved in this function (Supplementary Table 5). GO analysis for genes in the LN-associated "green" module did not demonstrate significant results. Pathways of KEGG analysis based on DEGs mostly correlated to LN in the "red" module were enriched in pathways responsible for virus infection and pattern recognition receptor signalings (Figure 5c), and details of this KEGG analysis were listed in Supplementary Table 6. No significant result was found in KEGG analysis in the IgAN-associated "salmon" module and the LN-associated "green" module.

With the use of Cytoscape, PPI networks of upregulated genes in common DEGs with the opposite-altered trend for IgAN and LN were constructed, respectively. The MCODE plug-in of Cytoscape was used to obtain the most closely related gene modules for IgAN and LN. Nine gene modules and seven gene modules were obtained for IgAN and LN, respectively. The gene modules consisting of risk factors in the nomograms were shown in Figure 5d and e. The other related modules were listed in Supplementary Figures 4 and 5.

Immune Infiltration Analysis and Its Correlation with Risk Factors in the Nomograms for IgAN and LN

Visualized results of the immune cell infiltration pattern of 22 types of leukocyte subpopulations in kidney tissues profiled by microarray in IgAN and LN were shown in Figure 6. Compared to HCs, the local infiltration of naive CD4+ T cells (p=0.03), regulatory T cells (p=0.02) and activated mast cells (p=0.04) was significantly more abundant while follicular helper T cells (p=0.05) and resting mast cells (p=0.03) infiltrated less (Figure 6a) in IgAN. Analysis in LN showed that the infiltration level of M2 macrophages (p=2.0e-5) increased significantly, while the infiltration level of M0 macrophages (p=0.01) and resting mast cells (p=0.05) in LN decreased significantly compared to HC (Figure 6b). And

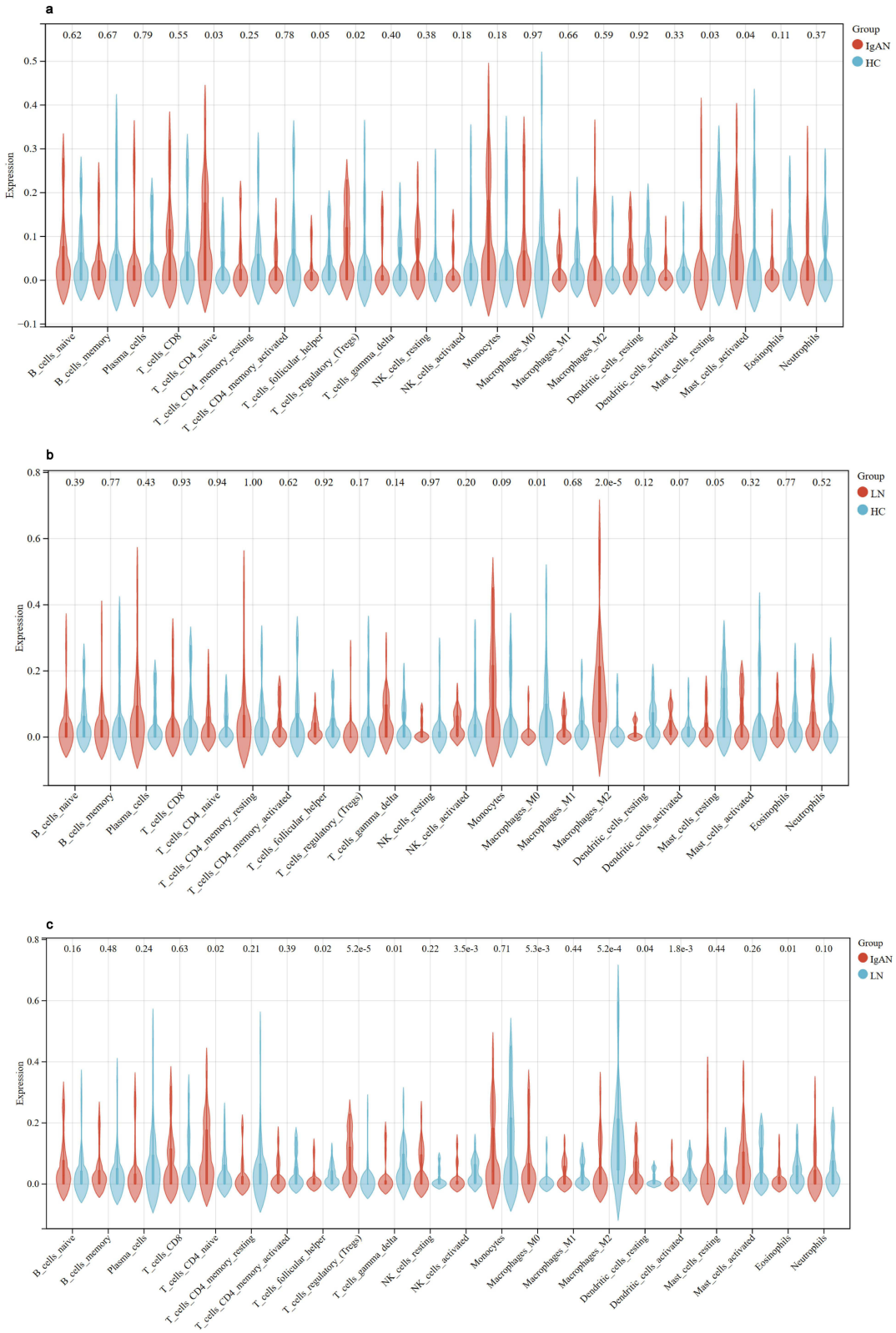

Figure 6 (**a**) Immune infiltration pattern in the glomerular compartment in IgAN patients compared to HCs. (**b**) Immune infiltration pattern in the glomerular compartment in LN patients compared to HCs. (**c**) Comparison of the immune infiltration pattern in the glomerular compartment between IgAN and LN patients.
Abbreviations: IgAN, immunoglobulin A nephropathy; LN, lupus nephritis; HC, healthy control.

comparison between IgAN and LN confirmed the distinct infiltration of CD4+ T cells, regulatory T cells, and M2 macrophages between IgAN and LN (Figure 6c). Analysis results of immune cell infiltration in IgAN and LN compared to HC were listed in Supplementary Table 7. In addition, RARG presented weakly correlation with infiltration of regulatory T cells in IgAN (r=0.33, p=0.02) while PRLH showed moderate correlation (r=0.46, p=9.55e-4), and HERC5 (r=0.66, p=1.02e-7) and ISG20 (r=0.61, p=1.70e-6) demonstrated strong correlation with M2 macrophages infiltration in LN (Figure 7).

Validation of the Independent Risk Genes for IgAN and LN by IHC

Figure 8 and Supplementary Figure 6 demonstrated the IHC staining results of RARG, PRLH, HERC5, and ISG20 in IgAN, LN, and HC. Characterized RARG staining in mesangial cells was detected in IgAN (median OD = 46.64 in IgAN vs 25.21 in LN; P = 0.0001), while PRLH staining was scattered in the glomeruli in IgAN, suggesting infiltrating inflammatory cells (median number of infiltrating cells = 11 in IgAN vs 1 in LN; P = 0.0008). Scattered staining of HERC5 indicating infiltrating inflammatory cells was also detected in the glomeruli in LN (median number of infiltrating cells = 0 in IgAN vs 9 in LN; P = 0.0003), while ISG20 showed linear staining in podocytes in LN (median OD = 2.82 in IgAN vs 15.76 in LN; P < 0.0001). IHC validated the independent risk genes in the nomograms for predicting differential diagnosis of IgAN and LN and revealed different expression profiles of those four genes.

Discussion

In this study, we investigated the common DEGs with opposite altered trends between IgAN and LN, and identified genes mostly correlated to IgAN and LN in the associated modules by WGCNA, respectively. Model construction using DEGs mostly correlated with IgAN and LN to predict differential diagnosis of IgAN and LN demonstrated that RARG and PRLH were independent risk factors for IgAN, and that HERC5 and ISG20 were independent risk factors for LN. GO analysis revealed that the DEGs are mostly correlated with IgAN in the "salmon" module mainly enriched in ligand-receptor activity-induced cellular growth and development, in which RARG and PRLH seem to play an indispensable role. HERC5 and ISG20 predicting LN participated in the nucleic acid/nucleotide binding-induced type I interferon-related activity and response to virus infection enriched in the biological function of DEGs mostly correlated with LN in the "red" module. IgAN and LN showed different immune cell infiltration patterns, in which HERC5 and ISG20 indicated a strong correlation with M2 macrophage infiltration, while the correlation between RARG and PRLH and

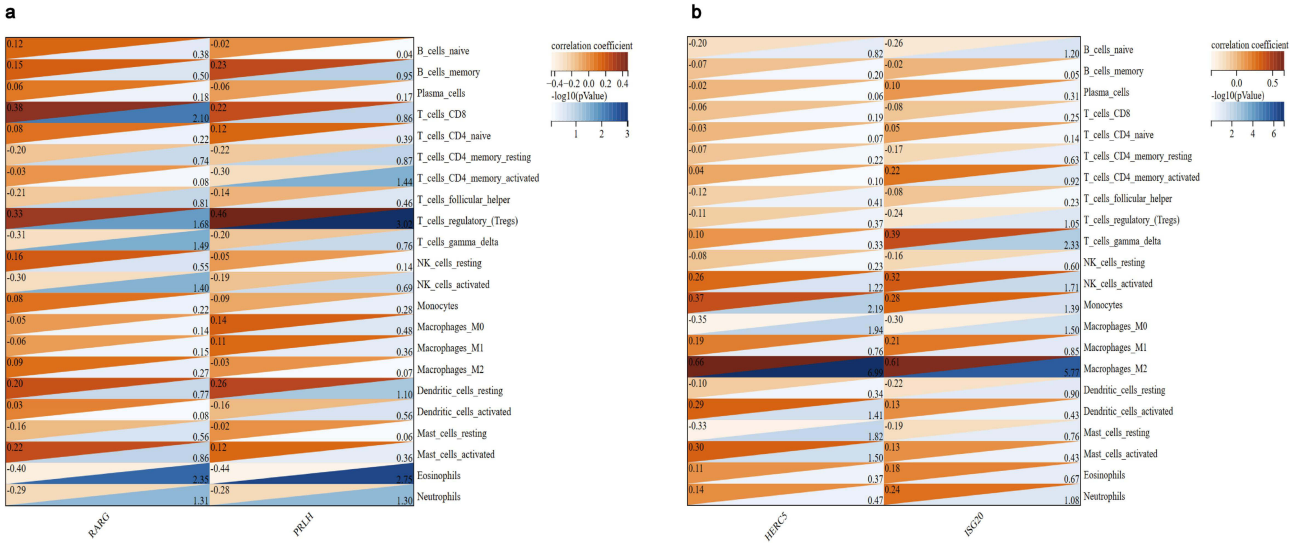

Figure 7 Result of correlation analysis of immune cell infiltration with risk factors genes in the nomograms predicting IgAN and LN. (**a**) The relationship between risk factor genes and immune cell infiltration in IgAN. (**b**) The relationship between risk factor genes and immune cell infiltration in LN.

Abbreviations: IgAN, immunoglobulin A nephropathy; LN, lupus nephritis; RARG, retinoic acid receptor γ; PRLH, prolactin releasing hormone; HERC5, HECT domain, and RCC1-like domain-containing protein 5; ISG20, interferon stimulated exonuclease gene 20.

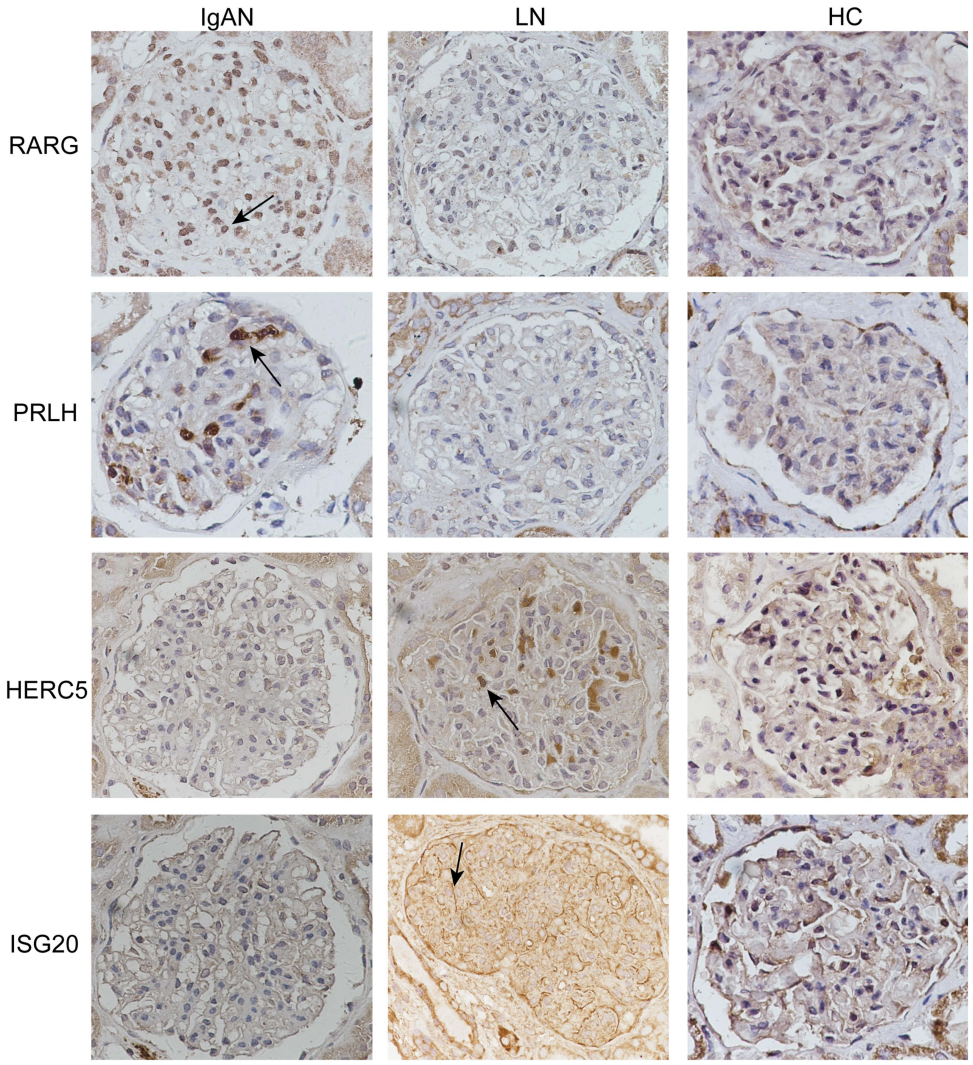

Figure 8 Validation of different expression patterns of RARG, PRLH, HERC5 and ISG20 in the predicting models for IgAN and LN by IHC.
Abbreviations: RARG, retinoic acid receptor γ; PRLH, prolactin releasing hormone; HERC5, HECT domain, and RCC1-like domain-containing protein 5; ISG20, interferon stimulated exonuclease gene 20; IgAN, immunoglobulin A nephropathy; LN, lupus nephritis; HC, healthy control; IHC, immunohistochemistry.

T-cell infiltration seemed to be weaker in IgAN. Further validation by IHC demonstrated different expression profiles of those four genes in the glomeruli in IgAN and LN.

Several studies have investigated the pathogenesis of IgAN and LN by bioinformatics analysis, respectively. Zhou[23] presented the result of GO enrichment in receptor-ligand activity in IgAN similar to our study. Wei[29] indicated an immune cell infiltration pattern in IgAN similar to ours with more abundance in CD4 naive T cells and regulatory T cells. However, diagnostic biomarkers at present for IgAN based on bioinformatics analysis seemed to be less convincing as they were not the results of WGCNA, LASSO regression and multivariate logistic analysis or laboratory validation.[21,23] Results of hub genes for LN including IFI44, IFIT3, HERC5, RSAD2, and DDX60, and biological function of type I interferon-related activity and response to virus infection enriched in GO analysis in previous studies[25,26] supported our findings in LN. Jia[28] demonstrated the first and the only one study comparing the expression profiles of IgAN and LN, but they mainly focused on the shared pathogenic modules of these two diseases enriched in immunity, cell death, and extracellular vesicle pathways, and explored the common disease–associated genetic variants in IgAN and LN in Asian and European populations by GWAS enrichment analysis. Our study remained the first one to explore the key differences in the pathogenic mechanisms between IgAN and LN.

The pathogenesis of IgAN is characterized by polyclonal Gd-IgA1 containing immune complex deposition-induced mesangial hypercellularity, extracellular matrix expansion, and release of cytokines attracting inflammatory cell infiltration. Gd-IgA1 containing immune complex could induce mesangial cell proliferation by binding to transferrin receptors (TfR1/CD71)[30] through the phosphoinositide 3-kinase (PI3K)/protein kinase B (Akt)/mammalian target of rapamycin (mTOR) pathway,[31,32] and the soluble Gd-IgA1 receptor FcαR (CD89) secreted by mesangial cells could enhance the above process by upregulating the expression of CD71 after binding to Gd-IgA1.[33,34] In addition, the Fcγ receptor on mesangial cells mediates phagocytosis of Gd-IgA1 containing immune complex.[35] The role of CD4+ T cells in IgAN has been well established by laboratory and clinical data, reviewed by Tang[8] and Ruszkowski[36] in detail. While both circulating Th1 and Th2 subsets increase in IgAN patients,[37] Th2 polarization in circulation seemed to dominate the immune abnormalities in IgAN in the chronic phase[38] and deteriorate renal fibrosis in IgAN,[39] and Th1 polarization occured in the early stage of the disease.[40] Th2 immune response promotion with increased levels of Th2 cytokines (IL-4 and IL-5) could induce abnormalities in the terminal glycosylation of IgA.[41,42] However, circulating regulatory T cell (Treg) has been reported to be significantly decreased and negatively correlated with clinical presentation in IgAN patients,[43] while our research demonstrated an abundance of Treg cells infiltrating the glomerular compartment. Th17 and Th22 cells were also involved in the immune response of IgAN.[44] Th17 cells could be recruited by CCL20 released by mesangial cells stimulated with IgA1 in an in vitro experiment.[45] The proliferative Th22 cells induced by increased IL-1, IL-6 and TNF-α level in hemolytic streptococcus infection were recruited by CCL20, CCL22, and CCL27 from mesangial cells and presented TGF-β, leading to renal fibrosis and progression in IgAN.[46] However, investigations of CD4+ T cells in the progression of IgAN were limited in their circulating components, and few studies have explored the function of infiltrating T cells in kidney in IgAN. Therefore, functional analysis of subpopulations of T cells infiltrating into intrarenal tissue in IgAN based on single-cell sequencing is urgently needed. According to the GeneCards database (https://www.genecards.org/), RARG we identified encodes a retinoic acid receptor belonging to the nuclear hormone receptor family and is associated with cellular growth and development. Retinoic acid signaling has been reported to promote IgAN through nuclear factor κB pathway[47] and enhance IgA class switch recombination.[48] Data from the Human Protein Atlas database (https://www.proteinatlas.org/) suggested that RARG expression was mostly enriched in fibroblasts (Supplementary Figure 7). As mesangial cells possess features of fibroblasts[49] and IHC in our study validated that RARG staining was mainly located in mesangial cells in the glomeruli, it is reasonable to hypothesize that RARG might be involved in the mesangial hypercellularity in IgAN. Such a hypothesis still needs further validation. The association between the expression of RARG and local infiltration of T cells expressing PRLH was weak, suggesting that the mesangial hypercellularity with highly expressed RARG was independent of T cell infiltration.

In SLE patients, delayed removal of dead cells originating from genetic defects results in misidentification of the self-nuclear antigens as viral nucleic acids by antigen-presenting cells, leading to induction of a type I interferon-mediated nonspecific antiviral response, and autoantibodies produced by autoreactive plasma cells targeting self-antigens induce immune complex deposition to initiate regional inflammation.[20] In LN, nucleic acids from different renal cells with different locations of immune complex deposition seem to be associated with different classes of pathologic changes in the kidney.[50,51] After stimulation by nucleic acids and the deposited immune complexes, renal cells produce massive amounts of type I interferon to promote the production of nuclear antigens by renal cells in turn, and autoantibodies then enhance the formation of immune complexes, induce inflammatory cells infiltration, and feedback to act on renal cells, leading to cellular injury and progression to renal fibrosis.[52,53] Type I interferon (IFN-β) induces macrophage infiltration by strongly enhancing the expression of chemokine (C-X-C motif) ligand 9 (CXCL9), CXCL10, and CXCL11.[54,55] Other chemokines inducing macrophage recruitment in LN mainly include monocyte chemotactic protein-1 (MCP-1), colony stimulating factor 1 (CSF-1), CXCL1, and osteopontin.[56] Renal biopsy specimens from LN patients suggested the dominant role of M2 macrophages rather than M1 macrophages in LN,[57] which was associated with complement activation.[58] Generally, M2 macrophages exert anti-inflammatory functions and protect against renal injury by secreting interleukin-10 (IL-10) and transforming growth factor-β (TGF-β). In LN patients, type I interferon could induce down-regulation of the anti-inflammatory heme oxygenase-1 with increased expression of IL-6 in M2 macrophages to enhance intrarenal inflammation,[59] which might be one of the reasons that M2 macrophage infiltration was associated with crescent formation in LN.[58,60] In a mouse model of LN, tissue-resident macrophages and monocyte-derived macrophages

have distinct pathogenic roles in expressing monocyte chemo-attractants and internalizing immune complexes, respectively, and similar grouped features of macrophages in renal tissue were also detected in kidney biopsies of LN patients, suggesting a division of labor in the kidney macrophage response in LN.[61] More details about the characteristics of macrophages in LN could be found in the review by Kwant.[56] According to the GeneCards database, HERC5 functions as an interferon-induced E3 protein ligase that mediates ISGylation of protein targets and also acts as a modulator of the antiviral immune response. ISG20 is involved in defense against virus, negative regulation of viral genome replication and nucleobase-containing compound catabolic process. HERC5 and ISG20 have been reported to be involved in the pathogenesis of LN.[25,26,62,63] Spotted HERC5 staining and linear staining of ISG20 in the podocytes in the IHC suggested the intraglomerular infiltrating macrophages and the podocyte injury in LN, respectively. However, the molecular mechanism of these two genes in deteriorating LN and the relationship between ISG20 associated podocyte injury and HERC5 associated macrophage activation still remained to be investigated.

Limitations in our study should be noted. First, we could not clarify the relationship between samples and clinical features as the data downloaded from the GEO database lacked the clinical information. And we chose IgAN and LN patients with similar mesangial hypercellularity and extracellular matrix expansion for the validated IHC for compensation. Second, the predicting models presented as nomograms we constructed were only used for differential diagnosis between IgAN and LN, and their efficacy in predicting the occurrence or the severity of these two diseases remained to be investigated. And as the data downloaded from the GEO database lacked the clinical information, there was no clinical data listed in the nomograms for prediction. Third, this study was carried out to explore the difference between IgAN and LN. We did not investigate the unique transcription characteristic of IgAN and/or LN for their diagnosis from other kidney diseases. Fourth, peripheral blood mononuclear cells of IgAN and LN patients should be acquired for another comparison study to fully elucidate the different mechanisms between the pathogenesis of IgAN and LN, and to validate the findings in our study. Fifth, more reliable experimental data to investigate the effect of RARG and PRLH in IgAN and the effect of HERC5 and ISG20 in LN are needed in the future.

Conclusion

Using bioinformatics technology, we demonstrated the key differences in the pathogenic mechanisms between IgAN and LN with the integrated gene expression profile of the renal glomerulus. RARG and PRLH served as biomarkers in predicting IgAN, and HERC5 and ISG20 were identified as biomarkers in predicting LN. Cellular growth and development characterized IgAN, while type I interferon-related activity and response to virus infection were the predominant features of LN. Different immune cell infiltration patterns between IgAN and LN were also investigated in this study. The differential expression pattern of those four genes for IgAN and LN prediction was validated by IHC, RARG and PRLH, HERC5, and ISG20 may play important roles in the pathogenesis of IgAN and LN, respectively. However, the effect of RARG and PRLH in IgAN and the effect of HERC5 and ISG20 in LN still need further investigation in the future.

Code Availability

: https://github.com/cran/WGCNA

Data Sharing Statement

The datasets analyzed during the current study are available in the Gene Expression Omnibus (GEO) datasets (http://www.ncbi.nlm.nih.gov/geo/).

Ethical Approval and Written Informed Consents

The study was conducted according to the guidelines of the Declaration of Helsinki and approved by the Ethics Committee of Peking University Third Hospital, approval number M2022204. Written informed consents were obtained from IgAN and LN patients to participate in the study if their renal biopsies were used for IHC.

Consent for Publication

All authors have approved for the publication of this manuscript.

Funding

This study was supported by grants from the National Natural Science Foundation of China (82070736) and the "PRO•Run" Fund of the Nephrology Group of CEBM.

Disclosure

The authors declare that they have no competing interests.

References

1. Schena FP, Nistor I. Epidemiology of IgA nephropathy: a global perspective. *Semin Nephrol*. 2018;38(5):435–442.
2. Hoover PJ, Costenbader KH. Insights into the epidemiology and management of lupus nephritis from the US rheumatologist's perspective. *Kidney Int*. 2016;90(3):487–492. doi:10.1016/j.kint.2016.03.042
3. Pattrapornpisut P, Avila-Casado C, Reich HN. IgA nephropathy: core curriculum 2021. *Am J Kidney Dis*. 2021;78(3):429–441. doi:10.1053/j.ajkd.2021.01.024
4. Gasparotto M, Gatto M, Binda V, et al. Lupus nephritis: clinical presentations and outcomes in the 21st century. *Rheumatology*. 2020;59(Suppl5):v39–v51. doi:10.1093/rheumatology/keaa381
5. Medjeral-Thomas NR, Cook HT, Pickering MC. Complement activation in IgA nephropathy. *Semin Immunopathol*. 2021;43(5):679–690. doi:10.1007/s00281-021-00882-9
6. Weinstein A, Alexander RV, Zack DJ. A review of complement activation in SLE. *Curr Rheumatol Rep*. 2021;23(3):16. doi:10.1007/s11926-021-00984-1
7. Li Y, Tang D, Yin L, et al. New insights for regulatory T cell in lupus nephritis. *Autoimmun Rev*. 2022;21(8):103134. doi:10.1016/j.autrev.2022.103134
8. Tang Y, He H, Hu P, et al. T lymphocytes in IgA nephropathy. *Exp Ther Med*. 2020;20(1):186–194. doi:10.3892/etm.2020.8673
9. Jing C, Castro-Dopico T, Richoz N, et al. Macrophage metabolic reprogramming presents a therapeutic target in lupus nephritis. *Proc Natl Acad Sci*. 2020;117(26):15160–15171. doi:10.1073/pnas.2000943117
10. Lv LL, Feng Y, Wen Y, et al. Exosomal CCL2 from tubular epithelial cells is critical for albumin-induced tubulointerstitial inflammation. *J Am Soc Nephrol*. 2018;29(3):919–935. doi:10.1681/ASN.2017050523
11. Conti F, Spinelli FR, Alessandri C, et al. Toll-like receptors and lupus nephritis. *Clin Rev Allergy Immunol*. 2011;40(3):192–198. doi:10.1007/s12016-010-8208-0
12. Coppo R, Amore A, Peruzzi L, et al. Innate immunity and IgA nephropathy. *J Nephrol*. 2010;23(6):626–632.
13. Coppo R, Troyanov S, Bellur S, et al. Validation of the Oxford classification of IgA nephropathy in cohorts with different presentations and treatments. *Kidney Int*. 2014;86(4):828–836. doi:10.1038/ki.2014.63
14. Trimarchi H, Barratt J, Cattran DC, et al. Oxford classification of IgA nephropathy 2016: an update from the IgA nephropathy classification working group. *Kidney Int*. 2017;91(5):1014–1021. doi:10.1016/j.kint.2017.02.003
15. Anders HJ. Nephropathic autoantigens in the spectrum of lupus nephritis. *Nat Rev Nephrol*. 2019;15(10):595–596. doi:10.1038/s41581-019-0168-x
16. Doria A, Gatto M. Nephritogenic-antinephritogenic antibody network in lupus glomerulonephritis. *Lupus*. 2012;21(14):1492–1496. doi:10.1177/0961203312462267
17. Perse M, Veceric-Haler Z. The role of IgA in the pathogenesis of IgA nephropathy. *Int J Mol Sci*. 2019;20(24):6199. doi:10.3390/ijms20246199
18. Knoppova B, Reily C, Maillard N, et al. The origin and activities of IgA1-containing immune complexes in IgA nephropathy. *Front Immunol*. 2016;7:117. doi:10.3389/fimmu.2016.00117
19. Leung JCK, Lai KN, Tang SCW. Role of mesangial-podocytic-tubular cross-talk in IgA nephropathy. *Semin Nephrol*. 2018;38(5):485–495. doi:10.1016/j.semnephrol.2018.05.018
20. Lech M, Anders HJ. The pathogenesis of lupus nephritis. *J Am Soc Nephrol*. 2013;24(9):1357–1366. doi:10.1681/ASN.2013010026
21. Qian W, Xiaoyi W, Zi Y. Screening and bioinformatics analysis of IgA nephropathy gene based on GEO databases. *Biomed Res Int*. 2019;2019:8794013. doi:10.1155/2019/8794013
22. Bai Y, Li Y, Xi Y, et al. Identification and validation of glomerulotubular crosstalk genes mediating IgA nephropathy by integrated bioinformatics. *BMC Nephrol*. 2022;23(1):143. doi:10.1186/s12882-022-02779-7
23. Zhou X, Wang N, Zhang Y, et al. Expression of CCL2, FOS, and JUN may help to distinguish patients with iga nephropathy from healthy controls. *Front Physiol*. 2022;13:840890. doi:10.3389/fphys.2022.840890
24. Chen Z, Lan R, Ye K, et al. Prioritization of diagnostic and prognostic biomarkers for lupus nephritis based on integrated bioinformatics analyses. *Front Bioeng Biotechnol*. 2021;9:717234. doi:10.3389/fbioe.2021.717234
25. Shen L, Lan L, Zhu T, et al. Identification and validation of IFI44 as key biomarker in lupus nephritis. *Front Med Lausanne*. 2021;8:762848. doi:10.3389/fmed.2021.762848
26. Wang L, Yang Z, Yu H, et al. Predicting diagnostic gene expression profiles associated with immune infiltration in patients with lupus nephritis. *Front Immunol*. 2022;13:839197. doi:10.3389/fimmu.2022.839197
27. Zhou X, Zhang Y, Wang N. Systematic identification of key extracellular proteins as the potential biomarkers in lupus nephritis. *Front Immunol*. 2022;13:915784. doi:10.3389/fimmu.2022.915784
28. Jia NY, Liu XZ, Zhang Z, et al. Weighted gene co-expression network analysis reveals different immunity but shared renal pathology between Iga nephropathy and lupus nephritis. *Front Genet*. 2021;12:634171. doi:10.3389/fgene.2021.634171
29. Wei SY, Guo S, Feng B, et al. Identification of miRNA-mRNA network and immune-related gene signatures in IgA nephropathy by integrated bioinformatics analysis. *BMC Nephrol*. 2021;22(1):392. doi:10.1186/s12882-021-02606-5
30. Jhee JH, Nam BY, Park JT, et al. CD71 mesangial IgA1 receptor and the progression of IgA nephropathy. *Transl Res*. 2021;230:34–43. doi:10.1016/j.trsl.2020.10.007

31. Tamouza H, Chemouny JM, Raskova Kafkova L, et al. The IgA1 immune complex-mediated activation of the MAPK/ERK kinase pathway in mesangial cells is associated with glomerular damage in IgA nephropathy. *Kidney Int*. 2012;82(12):1284–1296. doi:10.1038/ki.2012.192
32. Trimarchi H, Coppo R. Podocytopathy in the mesangial proliferative immunoglobulin A nephropathy: new insights into the mechanisms of damage and progression. *Nephrol Dial Transplant*. 2019;34(8):1280–1285. doi:10.1093/ndt/gfy413
33. Suzuki Y, Ra C, Saito K, et al. Expression and physical association of Fc alpha receptor and Fc receptor gamma chain in human mesangial cells. *Nephrol Dial Transplant*. 1999;14(5):1117–1123. doi:10.1093/ndt/14.5.1117
34. Berthelot L, Papista C, Maciel TT, et al. Transglutaminase is essential for IgA nephropathy development acting through IgA receptors. *J Exp Med*. 2012;209(4):793–806. doi:10.1084/jem.20112005
35. Santiago A, Mori T, Satriano J, et al. Regulation of Fc receptors for IgG on cultured rat mesangial cells. *Kidney Int*. 1991;39(1):87–94. doi:10.1038/ki.1991.11
36. Ruszkowski J, Lisowska KA, Pindel M, et al. T cells in IgA nephropathy: role in pathogenesis, clinical significance and potential therapeutic target. *Clin Exp Nephrol*. 2019;23(3):291–303. doi:10.1007/s10157-018-1665-0
37. Lai KN, Ho RT, Lai CK, et al. Increase of both circulating Th1 and Th2 T lymphocyte subsets in IgA nephropathy. *Clin Exp Immunol*. 1994;96(1):116–121. doi:10.1111/j.1365-2249.1994.tb06240.x
38. Ebihara I, Hirayama K, Yamamoto S, et al. Th2 predominance at the single-cell level in patients with IgA nephropathy. *Nephrol Dial Transplant*. 2001;16(9):1783–1789. doi:10.1093/ndt/16.9.1783
39. Liu L, Kou P, Zeng Q, et al. CD4+ T Lymphocytes, especially Th2 cells, contribute to the progress of renal fibrosis. *Am J Nephrol*. 2012;36(4):386–396. doi:10.1159/000343283
40. Suzuki H, Suzuki Y. Murine models of human IgA nephropathy. *Semin Nephrol*. 2018;38(5):513–520. doi:10.1016/j.semnephrol.2018.05.021
41. Chintalacharuvu SR, Emancipator SN. The glycosylation of IgA produced by murine B cells is altered by Th2 cytokines. *J Immunol*. 1997;159(5):2327–2333. doi:10.4049/jimmunol.159.5.2327
42. Chintalacharuvu SR, Yamashita M, Bagheri N, et al. T cell cytokine polarity as a determinant of immunoglobulin A (IgA) glycosylation and the severity of experimental IgA nephropathy. *Clin Exp Immunol*. 2008;153(3):456–462. doi:10.1111/j.1365-2249.2008.03703.x
43. Huang H, Sun W, Liang Y, et al. CD4 (+)CD 25 (+)Treg cells and IgA nephropathy patients with tonsillectomy: a clinical and pathological study. *Int Urol Nephrol*. 2014;46(12):2361–2369. doi:10.1007/s11255-014-0851-6
44. Peng Z, Tian J, Cui X, et al. Increased number of Th22 cells and correlation with Th17 cells in peripheral blood of patients with IgA nephropathy. *Hum Immunol*. 2013;74(12):1586–1591. doi:10.1016/j.humimm.2013.08.001
45. Lu G, Zhang X, Shen L, et al. CCL20 secreted from IgA1-stimulated human mesangial cells recruits inflammatory Th17 cells in IgA nephropathy. *PLoS One*. 2017;12(5):e0178352. doi:10.1371/journal.pone.0178352
46. Gan L, Zhou Q, Li X, et al. Intrinsic renal cells induce lymphocytosis of Th22 cells from IgA nephropathy patients through B7-CTLA-4 and CCL-CCR pathways. *Mol Cell Biochem*. 2018;441(1–2):191–199. doi:10.1007/s11010-017-3185-8
47. Moller-Hackbarth K, Dabaghie D, Charrin E, et al. Retinoic acid receptor responder1 promotes development of glomerular diseases via the Nuclear Factor-kappaB signaling pathway. *Kidney Int*. 2021;100(4):809–823. doi:10.1016/j.kint.2021.05.036
48. He L, Peng X, Chen Y, et al. Regulation of IgA Class Switch Recombination in Immunoglobulin A Nephropathy: retinoic Acid Signaling and BATF. *Am J Nephrol*. 2016;43(3):179–194. doi:10.1159/000445697
49. He B, Chen P, Zambrano S, et al. Single-cell RNA sequencing reveals the mesangial identity and species diversity of glomerular cell transcriptomes. *Nat Commun*. 2021;12(1):2141. doi:10.1038/s41467-021-22331-9
50. Weening JJ, D'Agati VD, Schwartz MM, et al. The classification of glomerulonephritis in systemic lupus erythematosus revisited. *Kidney Int*. 2004;65(2):521–530. doi:10.1111/j.1523-1755.2004.00443.x
51. Mortensen ES, Rekvig OP. Nephritogenic potential of anti-DNA antibodies against necrotic nucleosomes. *J Am Soc Nephrol*. 2009;20(4):696–704. doi:10.1681/ASN.2008010112
52. Ding X, Ren Y, He X. IFN-I mediates lupus nephritis from the beginning to renal fibrosis. *Front Immunol*. 2021;12:676082. doi:10.3389/fimmu.2021.676082
53. Lorenz G, Anders HJ. Neutrophils, dendritic cells, toll-like receptors, and interferon-alpha in lupus nephritis. *Semin Nephrol*. 2015;35(5):410–426. doi:10.1016/j.semnephrol.2015.08.003
54. Triantafyllopoulou A, Franzke CW, Seshan SV, et al. Proliferative lesions and metalloproteinase activity in murine lupus nephritis mediated by type I interferons and macrophages. *Proc Natl Acad Sci*. 2010;107(7):3012–3017. doi:10.1073/pnas.0914902107
55. Groom JR, Luster AD. CXCR3 in T cell function. *Exp Cell Res*. 2011;317(5):620–631. doi:10.1016/j.yexcr.2010.12.017
56. Kwant LE, Vegting Y, Tsang ASMWP, et al. Macrophages in lupus nephritis: exploring a potential new therapeutic avenue. *Autoimmun Rev*. 2022;21(12):103211. doi:10.1016/j.autrev.2022.103211
57. Olmes G, Buttner-Herold M, Ferrazzi F, et al. CD163+ M2c-like macrophages predominate in renal biopsies from patients with lupus nephritis. *Arthritis Res Ther*. 2016;18(1):90. doi:10.1186/s13075-016-0989-y
58. Tao J, Zhao J, Qi XM, et al. Complement-mediated M2/M1 macrophage polarization may be involved in crescent formation in lupus nephritis. *Int Immunopharmacol*. 2021;101(Pt A):108278. doi:10.1016/j.intimp.2021.108278
59. Kishimoto D, Kirino Y, Tamura M, et al. Dysregulated heme oxygenase-1(low) M2-like macrophages augment lupus nephritis via Bach1 induced by type I interferons. *Arthritis Res Ther*. 2018;20(1):64. doi:10.1186/s13075-018-1568-1
60. Li J, Yu YF, Liu CH, et al. Significance of M2 macrophages in glomerulonephritis with crescents. *Pathol Res Pract*. 2017;213(9):1215–1220. doi:10.1016/j.prp.2017.04.011
61. Richoz N, Tuong ZK, Loudon KW, et al. Distinct pathogenic roles for resident and monocyte-derived macrophages in lupus nephritis. *JCI Insight*. 2022;7(21). doi:10.1172/jci.insight.159751
62. Coit P, Renauer P, Jeffries MA, et al. Renal involvement in lupus is characterized by unique DNA methylation changes in naive CD4+ T cells. *J Autoimmun*. 2015;61:29–35. doi:10.1016/j.jaut.2015.05.003
63. Pan HF, Leng RX, Feng CC, et al. Expression profiles of Th17 pathway related genes in human systemic lupus erythematosus. *Mol Biol Rep*. 2013;40(1):391–399. doi:10.1007/s11033-012-2073-2